

Cu(I)-SNS complexes for outer-sphere hydroboration and hydrosilylation of carbonyls

Matthew R. Elsby and R. Tom Baker*

Department of Chemistry and Biomolecular Sciences and Centre for Catalysis
Research and Innovation, University of Ottawa, Ottawa, Ontario K1N 6N5, Canada

Electronic Supporting Information:

Table of Contents:

S2 – General Considerations

S3 – Synthesis and Characterization of Copper Complexes

S6 – Procedures for Hydrosilylation & Hydroboration Catalysis

S9 – Mechanistic Studies

S11 – NMR Spectra

S24 – X-ray Diffraction Data

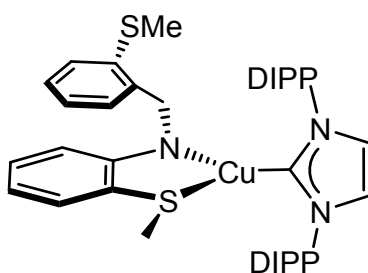
S29 – References

General Considerations.

Unless otherwise stated, all reactions were carried out under an atmosphere of dry, oxygen-free dinitrogen by means of standard Schlenk or glovebox techniques. Benzene- d_6 was degassed by three freeze-pump-thaw cycles, and subsequently dried by running through a column of activated alumina. Toluene, hexanes, and THF were dried on columns of activated alumina using a J. C. Meyer (formerly Glass Contour) solvent purification system. ^1H NMR spectra were recorded on either a Bruker Avance, Avance II, or Avance III Spectrometer operating at either 300 or 500 MHz with respect to proton nuclei. ^1H NMR spectra were referenced to residual protons (C_6D_6 , δ 7.15) with respect to tetramethylsilane at δ 0.00. $^{13}\text{C}\{^1\text{H}\}$ NMR spectra were referenced relative to solvent resonance (C_6D_6 , δ 127.2). Abbreviations: s-singlet, d-doublet, tr-triplet, sept-septet, ov-overlapping, mult-multiplet, br-broad. All reagents were purchased from commercial suppliers. The compounds DBpin,¹ CuCl(IPr),² **L1**,³ and **L2**⁴ were all prepared according to literature procedures.

Synthesis of [Cu(S^{Me}NS^{Me})(IPr) [Cu-1]. A vial equipped with a magnetic stir bar was charged with CuCl(IPr) (0.097 g, 0.199 mmol) and dissolved in 3 mL of THF. A 3 mL THF solution of **L1** (0.055 g, 0.199 mmol) and LiHMDS (0.033 g, 0.199 mmol) was added dropwise to the reaction mixture while stirring, resulting in a bright yellow solution that was stirred for 18 h. The solution was evaporated in vacuo, washed with hexanes, and further dried. The residue was extracted into toluene, filtered through Celite, and concentrated in vacuo to yield a pale-yellow powder (0.133 g, 92% yield). X-ray quality crystals were grown from a concentrated solution in toluene layered with hexanes at -30 °C. **^1H NMR (C_6D_6 , 23 °C, 500 MHz):** δ 1.04 (d, 12H, CH-(CH₃)₂, $^3J_{\text{HH}} = 7.0$ Hz); 1.31 (d,

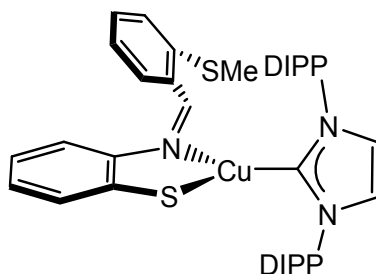
12H, CH-(CH₃)₂, ³J_{HH} = 7.0 Hz); 1.61 (s, 3H, S-CH₃); 2.15 (s, 3H, S-CH₃); 2.72 (sept, 4H, CH-(CH₃)₂, ³J_{HH} = 7.0 Hz); 4.39 (s, 2H, N=CH₂); 6.25 (dd, 1H, Ar-H, ³J_{HH} = 8.5 Hz, ⁴J_{HH} = 1.0 Hz); 6.30 (ddd, 1H, Ar-H, ³J_{HH} = 8.5, 7.5 Hz, ⁴J_{HH} = 1.5 Hz); 6.36 (s, 2H, HC=CH); 6.82 (ddd, 1H, Ar-H, ³J_{HH} = 7.5, 7.5 Hz, ⁴J_{HH} = 1.5 Hz); 6.89 (ddd, 1H, Ar-H, ³J_{HH} = 8.5, 7.5 Hz, ⁴J_{HH} = 1.5 Hz); 7.02 (ov dd, 1H, Ar-H, ⁴J_{HH} = 1.5 Hz); 7.04 (m, 4H, Ph-H); 7.06 (ov ddd, 1H, Ar-H, ³J_{HH} = 7.5, 7.5 Hz, ⁴J_{HH} = 1.5 Hz); 7.17 (m, 2H, Ph-H); 7.29 (dd, 1H, Ar-H, ³J_{HH} = 7.5 Hz, ⁴J_{HH} = 1.0 Hz); 7.41 (dd, 1H, Ar-H, ³J_{HH} = 7.5 Hz, ⁴J_{HH} = 1.5 Hz). ¹³C{¹H} NMR (C₆D₆, 23 °C, 500 MHz): δ 14.9 (s, 1C, S-CH₃); 19.8 (s, 1C, S-CH₃); 23.7 (s, 4C, CH-CH₃); 23.8 (s, 4C, CH-CH₃); 28.5 (s, 4C, CH-CH₃); 53.6 (s, 1C, N-CH₂); 109.5 (s, 1C, Ar_{SNS}-C); 111.4 (s, 1C, Ar_{SNS}-C); 118.1 (s, 1C, Ar_{SNS}-C); 121.7 (s, 2C, HC=CH); 123.8 (s, 1C, Ph-C); 124.1 (s, 1C, Ar_{SNS}-C); 124.3 (s, 1C, Ar_{SNS}-C); 125.2 (s, 1C, Ar_{SNS}-C); 126.6 (s, 1C, Ar_{SNS}-C); 129.6 (s, 1C, Ar_{SNS}-C); 129.7 (s, 1C, Ph-C); 132.8 (s, 1C, Ar_{SNS}-C); 135.9 (s, 1C, Ar_{SNS}-C); 141.2 (s, 1C, Ar_{SNS}-C); 145.2 (s, 1C, Ph-C); 159.2 (s, 1C, Ph-C); 186.8 (s, 1C, Cu-C). Calcd for C₄₂H₅₃Cu N₃S₂: %C 69.33; %H 7.34; %N 5.78. Found: %C 69.38; %H 7.04; %N 5.46.



Synthesis of Cu(S^{Me}NS)(IPr) [Cu-2]. In a vial charged with a magnetic stir bar, CuCl(IPr) (0.141 g, 0.289 mmol) and **L2** (0.075 g, 0.289 mmol) were dissolved in 3 mL of toluene giving a dark brown solution. While stirring, potassium tert-butoxide (0.032 g, 0.289 mmol) was slowly added over one min, resulting in an immediate color change to dark red. The

solution was stirred at room temperature for 6 h, filtered through Celite and concentrated in vacuo. The resulting solid was washed with hexanes and further dried, resulting in a dark red solid (0.180 g, 88% yield). X-ray quality crystals were grown from a concentrated toluene solution layered with hexanes at room temperature. **¹H NMR (C₆D₆, 23 °C, 300 MHz):** Isomer #1: δ 1.11 (d, 12H, CH-(CH₃)₂, ³J_{HH} = 7.0 Hz); 1.49 (d, 12H, CH-(CH₃)₂, ³J_{HH} = 7.0 Hz); 2.02 (s, 3H, S-CH₃); 2.86 (sept, 4H, CH-(CH₃)₂, ³J_{HH} = 7.0 Hz); 6.28 (ddd, 1H, Ar-H, ³J_{HH} = 8, 7 Hz, ⁴J_{HH} = 1.5 Hz); 6.43 (ov dd, 1H, Ar-H, ³J_{HH} = 7 Hz, ⁴J_{HH} = 1.5 Hz); 6.44 (s, 2H, HC=CH); 6.65 (ddd, 1H, Ar-H, ³J_{HH} = 8, 7 Hz, ⁴J_{HH} = 1.5 Hz); 6.70 (ddd, 1H, Ar-H, ³J_{HH} = 8, 7 Hz, ⁴J_{HH} = 1.5 Hz); 6.77 (dd, 1H, Ar-H, ³J_{HH} = 7 Hz, ⁴J_{HH} = 1.5 Hz); 6.80 (ov m, 1H, Ar-H); 6.90 (ddd, 1H, Ar-H, ³J_{HH} = 7, 7 Hz, ⁴J_{HH} = 1.5 Hz); 7.10 (m, 4H, Ph-H); 7.18 (m, 2H, Ph-H); 7.40 (s, 1H, N=CH); 7.81 (dd, 1H, Ar-H, ³J_{HH} = 8 Hz, ⁴J_{HH} = 1.5 Hz). Isomer #2: δ 1.03 (d, 12H, CH-(CH₃)₂, ³J_{HH} = 7.0 Hz); 1.26 (d, 12H, CH-(CH₃)₂, ³J_{HH} = 7.0 Hz); 1.89 (s, 3H, S-CH₃); 2.73 (br sept, 4H, CH-(CH₃)₂, ³J_{HH} = 7.0 Hz); 6.34 (ov mult, 1H, Ar-H); 6.34 (s, 2H, HC=CH); 6.78 (ov mult, 4H, Ar-H); 6.85 (dmult, 1H, Ar-H, ³J_{HH} = 8.0 Hz); 7.05 (mult, 4H, Ph-H); 7.18 (mult, 2H, Ph-H); 7.32 (br mult, 1H, Ar-H); 8.03 (br mult, 1H, Ar-H); 8.60 (s, 1H, N=CH). **¹³C{¹H} NMR (C₆D₆, 23 °C, 300 MHz):** Isomer #1: δ 15.8 (s, 1C, S-CH₃); 24.0 (s, 4C, CH-CH₃); 24.2 (s, 4C, CH-CH₃); 28.7 (s, 4C, CH-CH₃); 121.7 (s, 2C, HC=CH); 124.0, 129.8, 145.5, 154.3 (s, Ph-C); 118.9, 119.9, 125.5, 126.4, 129.0, 129.8, 135.3, 135.9, 137.7, 147.5, 151.1 (s, 1C, Ar_{SNS}-C); 133.0 (s, 1C, N=C); 187.2 (s, 1C, Cu-C). Isomer #2: δ 13.9 (s, 1C, S-CH₃); 23.7 (s, 4C, CH-CH₃); 24.1 (s, 4C, CH-CH₃); 28.6 (s, 4C, CH-CH₃); 122.0 (s, 2C, HC=CH); 123.8, 129.9, 145.5, 155.0 (s, Ph-C); 117.8, 120.3, 125.4, 126.2, 129.1, 129.6, 135.0, 136.3, 138.2, 146.6,

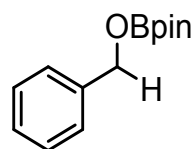
152.3 (s, 1C, Ar_{SNS}-C); 125.1 (s, 1C, N=C); 185.7 (s, 1C, Cu-C). Calcd for C₄₁H₄₉CuN₃S₂: %C 69.21; %H 6.94; %N 5.91. Found: %C 68.81; %H 7.43; %N 5.32.



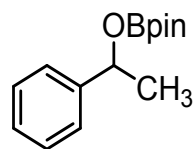
General Procedure 'A' for Hydroboration of Carbonyls. A stock solution of **Cu-1/Cu-2** was prepared by dissolving the appropriate Cu-complex (10 mg) in C₆D₆ (2 mL). A vial containing **Cu-1/Cu-2** (0.001 g, 20 μ l, 0.001 mmol, 1 mol%) in 0.6 g of C₆D₆ was charged first with the appropriate substrate, and subsequently with pinacolborane, resulting in an immediate color change from pale-yellow to colorless. The solution was charged to an NMR tube for further analysis. Reaction times varied slightly from 2-10 minutes. Yield was determined by ¹H NMR in reference to internal standard mesitylene.

General Procedure 'B' for Hydrosilylation of Carbonyls. A stock solution of **Cu-1** was prepared by dissolving the appropriate Cu-complex (10 mg) in C₆D₆ (2 mL). A vial containing **Cu1** (0.001 g, 20 μ l, 0.001 mmol, 1 mol%) in 0.6 g of C₆D₆ was charged first with the appropriate substrate, and subsequently with triethoxysilane, resulting in an immediate color change from pale-yellow to dark yellow. The solution was charged to an NMR tube for further analysis. Reaction times varied slightly from 2-10 minutes. Yield was determined by ¹H NMR in reference to internal standard mesitylene.

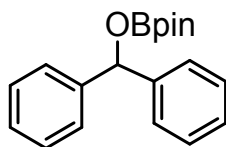
Hydroboration of benzaldehyde. Carried out according to *General Procedure A* using benzaldehyde (0.015 g, 14 μ l, 0.142 mmol), pinacolborane (0.018 g, 20 μ l, 0.142 mmol), and either **Cu-1** (0.001 g, 20 μ l, 0.001 mmol, 1 mol %), or **Cu-2** (0.001 g, 20 μ l, 0.001 mmol, 1 mol %). ^1H NMR showed quantitative conversion to hydroboration product after 5 min at room temperature. ^{11}B and ^1H NMR shifts matched with literature values.⁵



Hydroboration of acetophenone. Conducted according to *General Procedure A* using acetophenone (0.017 g, 16 μ l, 0.142 mmol), pinacolborane (0.018 g, 20 μ l, 0.142 mmol), and **Cu-1** (0.001 g, 20 μ l, 0.001 mmol, 1 mol %), or **Cu-2** (0.001 g, 20 μ l, 0.001 mmol, 1 mol %). ^1H NMR showed quantitative conversion to hydroboration product after 5 min at room temperature. ^{11}B and ^1H NMR shifts matched with literature values.⁵

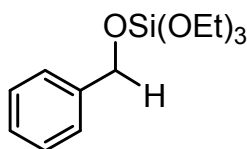


Hydroboration of benzophenone. Conducted according to *General Procedure A* using benzophenone (0.025 g, 0.142 mmol), pinacolborane (0.018 g, 20 μ l, 0.142 mmol), and **Cu-1** (0.001 g, 20 μ l, 0.001 mmol, 1 mol %), or **Cu-2** (0.001 g, 20 μ l, 0.001 mmol, 1 mol %). ^1H NMR showed quantitative conversion to hydroboration product after 10 min at room temperature. ^{11}B and ^1H NMR shifts matched with literature values.⁵

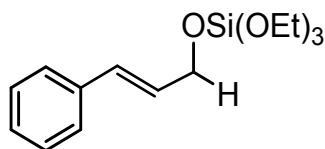


Hydrosilylation of benzaldehyde with Cu-1. Carried out according to *General Procedure B* using benzaldehyde (0.015 g, 14 μ l, 0.142 mmol), triethoxysilane (0.023 g, 26 μ l, 0.142 mmol), and **Cu-1** (0.001 g, 20 μ l, 0.001 mmol, 1 mol %). ^1H NMR showed

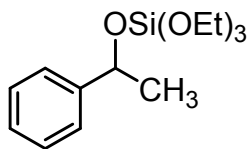
quantitative conversion to hydrosilylation product after 5 min at room temperature. ^1H NMR shifts matched with literature values.⁶



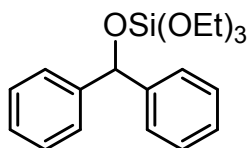
Hydrosilylation of *trans*-cinnamaldehyde with Cu-1. Synthesized according to *General Procedure B* using *trans*-cinnamaldehyde (0.018 g, 17 μl , 0.142 mmol), triethoxysilane (0.023 g, 26 μl , 0.142 mmol), and **Cu-1** (0.001 g, 20 μl , 0.001 mmol, 1 mol %). ^1H NMR showed 92% yield in reference to internal standard mesitylene to hydrosilylation product after 5 min at room temperature. ^1H NMR shifts matched with literature values.⁷ After 24 h, we noticed significant *cis-trans* equilibration in the reaction solution Figure S10b and an unidentified impurity was also present (Figure S10).



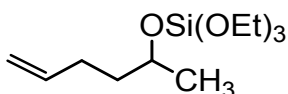
Hydrosilylation of acetophenone with Cu-1. Conducted according to *General Procedure B* using acetophenone (0.017 g, 16 μl , 0.142 mmol), triethoxysilane (0.023 g, 26 μl , 0.142 mmol), and **Cu-1** (0.001 g, 20 μl , 0.001 mmol, 1 mol %). ^1H NMR showed quantitative conversion to hydrosilylation product after 5 min at room temperature. ^1H NMR shifts matched with literature values.⁸



Hydrosilylation of benzophenone with Cu-1. Carried out according to *General Procedure B* using benzophenone (0.025 g, 0.142 mmol), triethoxysilane (0.023 g, 26 μl , 0.142 mmol), and **Cu-1** (0.001 g, 20 μl , 0.001 mmol, 1 mol %). ^1H NMR showed quantitative conversion to hydrosilylation product after 10 min at room temperature. ^1H NMR shifts matched with literature values.⁹



Hydrosilylation of 5-hexen-2-one with Cu-1. Conducted according to *General Procedure B* using 5-hexen-2-one (0.013 g, 16 μ l, 0.142 mmol), triethoxysilane (0.023 g, 26 μ l, 0.142 mmol), and **Cu-1** (0.001 g, 20 μ l, 0.001 mmol, 1 mol %). ^1H NMR showed quantitative conversion to hydrosilylation product after 10 min at room temperature. ^1H NMR shifts were similar to the known trimethylsilylether analogue.¹⁰ **^1H NMR (C_6D_6 , 23 $^\circ\text{C}$, 300 MHz):** δ 1.17 (tr, 9H, OCH_2CH_3 , $^3J_{\text{HH}} = 7$ Hz); 1.23 (d, 3H, $\text{Si}(\text{C})(\text{CH}_3)$, $^3J_{\text{HH}} = 6$ Hz); 1.48 (second order mult, 1H); 1.68 (second order mult, 1H, $\text{Si}(\text{C})(\text{CH}_2)(\text{CH}_2)$); 2.18 (second order mult, 1H, $\text{Si}(\text{C})(\text{CH}_2)$, $^3J_{\text{HH}} = 6$ Hz); 3.86 (q, 6H, OCH_2CH_3 , $^3J_{\text{HH}} = 7$ Hz); 4.16 (second order mult, 1H, $\text{Si}(\text{C})(\text{CH}_2)$, $^3J_{\text{HH}} = 6$ Hz); 4.97 (dmult, 1H, $=\text{CH}_2$, $^3J_{\text{HH}} = 10$ Hz); 5.06 (dmult, 1H, $=\text{CH}_2$, $^3J_{\text{HH}} = 17$ Hz); 5.81 (second order mult, 1H, $=\text{CH}$, $^3J_{\text{HH}} = 17$, 10 Hz).



Attempted hydrosilylation of benzaldehyde with Cu-2. Carried out according to *General Procedure B* using acetophenone (0.017 g, 16 μ l, 0.142 mmol), triethoxysilane (0.023 g, 26 μ l, 0.142 mmol), and **Cu-2** (0.001 g, 20 μ l, 0.001 mmol, 1 mol %). Crude ^1H NMR spectrum after 1 h showed no product formation. Decomposition was observed after 24 h. Attempts to heat above 50 $^\circ\text{C}$ resulted in immediate decomposition.

Attempted hydrosilylation of acetophenone with Cu-2. Conducted according to *General Procedure B* using benzaldehyde (0.015 g, 14 μ l, 0.142 mmol), triethoxysilane (0.023 g, 26 μ l, 0.142 mmol), and **Cu-2** (0.001 g, 20 μ l, 0.001 mmol, 1 mol %). Crude ^1H NMR after 1 h showed no product formation. Decomposition was observed after 24 h. Attempts to heat above 50 $^\circ\text{C}$ resulted in immediate decomposition.

Mechanistic Studies

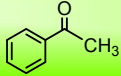
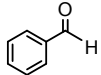
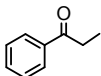
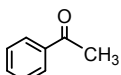
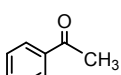
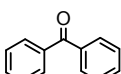
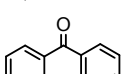
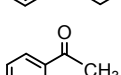
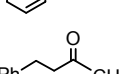
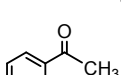
Stoichiometric Reaction of Cu-1 with HBpin. A pale-yellow solution of **Cu-1** (0.01 g, 0.014 mmol) in C_6D_6 was charged with pinacolborane (0.002 g, 2 μ l, 0.014 mmol), resulting in an immediate color change to deep yellow. The crude 1H NMR spectrum showed complete consumption of **Cu-1** into a new copper-hydride species. Continual monitoring showed decomposition after 2 h at room temperature as evidenced by free **L1** appearing in the 1H NMR spectrum (*Figures S14 and S15*).

Stepwise Hydroboration of acetophenone with Cu-1. The reaction detailed above was repeated to generate the deep yellow solution of copper-hydride. To investigate if this species is an intermediate in a catalytic cycle, acetophenone (0.002, 1.6 μ l, 0.014 mmol) was added to the solution resulting in an immediate color change to pale yellow. The crude 1H NMR spectrum showed the growth of both hydroboration product, and the regeneration of **Cu-1** (*Figure S14*).

Stoichiometric Reaction of Cu-2 with HBpin. A dark red solution of **Cu-2** (0.015 g, 0.021 mmol) in C_6D_6 was charged with pinacolborane (0.003 g, 3 μ l, 0.021 mmol), resulting in an immediate color change to orange, and then pale yellow. Crude 1H NMR showed the complete consumption of **Cu-2** into multiple isomers of a new species with no obvious potential hydride resonances (*Figures S16 and S17*).

Stoichiometric Reaction of Cu-1 with DBpin. A C_6D_6 solution of DBpin (0.003g, 0.021 mmol) was charged to a vial containing **Cu-1** (0.015g, 0.021 mmol) resulting in a deep yellow solution. Observation of the 1H NMR spectrum showed the absence of a singlet at 2.3 ppm as seen in the previous reaction with HBpin. Attempts to observe the Cu–D were unsuccessful due to the signal being drowned out by C_6D_6 .

Table S1. Survey of most efficient Cu-catalyzed hydrosilylation of carbonyls.

Catalyst	mol %	Substrate	Additives	Silane (equiv.)	Time/temp	Yield(%)	ref
[Cu(S ^{Me} NS ^{Me})(IPr)]	0.1		none	(OEt) ₃ SiH(1)	5 min, rt	>99	
[Cu(H)(PPh ₃)]	3		none	Ph ₂ MeSiH (2.5)	120 min, rt	98	11
[Cu(H)(PPh ₃)]	3		none	PMHS (2.5)	10 h, rt	97	11
[CuF ₂] / (S)-BINAP	4		none	Ph ₃ SiH (1.5)	2 h, rt	98	12
[Cu(Cl)(IPr)]	3		NaO ^t Bu (12%)	Et ₃ SiH (3)	3 h, rt	98	13
CuCl / IPr•HBF ₄	3		NaO ^t Bu (20%)	Et ₃ SiH (5)	8 h, 80°C	100	14
[Cu(Cl)(ICy)]	3		NaO ^t Bu (12%)	Et ₃ SiH (3)	25 min, 80°C	99	14
[(IPr) ₂ Cu] BF ₄	3		NaO ^t Bu (12%)	Et ₃ SiH (2)	4 h, rt	98	15
(IMes) ₂ CuF•HF	5		none	Me(OEt) ₂ SiH(1.5)	25 min, rt	>99	16
Cu(OAc) ₂ / (S)-BINAP	3		none	Ph ₃ SiH (1.2)	7 h, 0°C	94	17

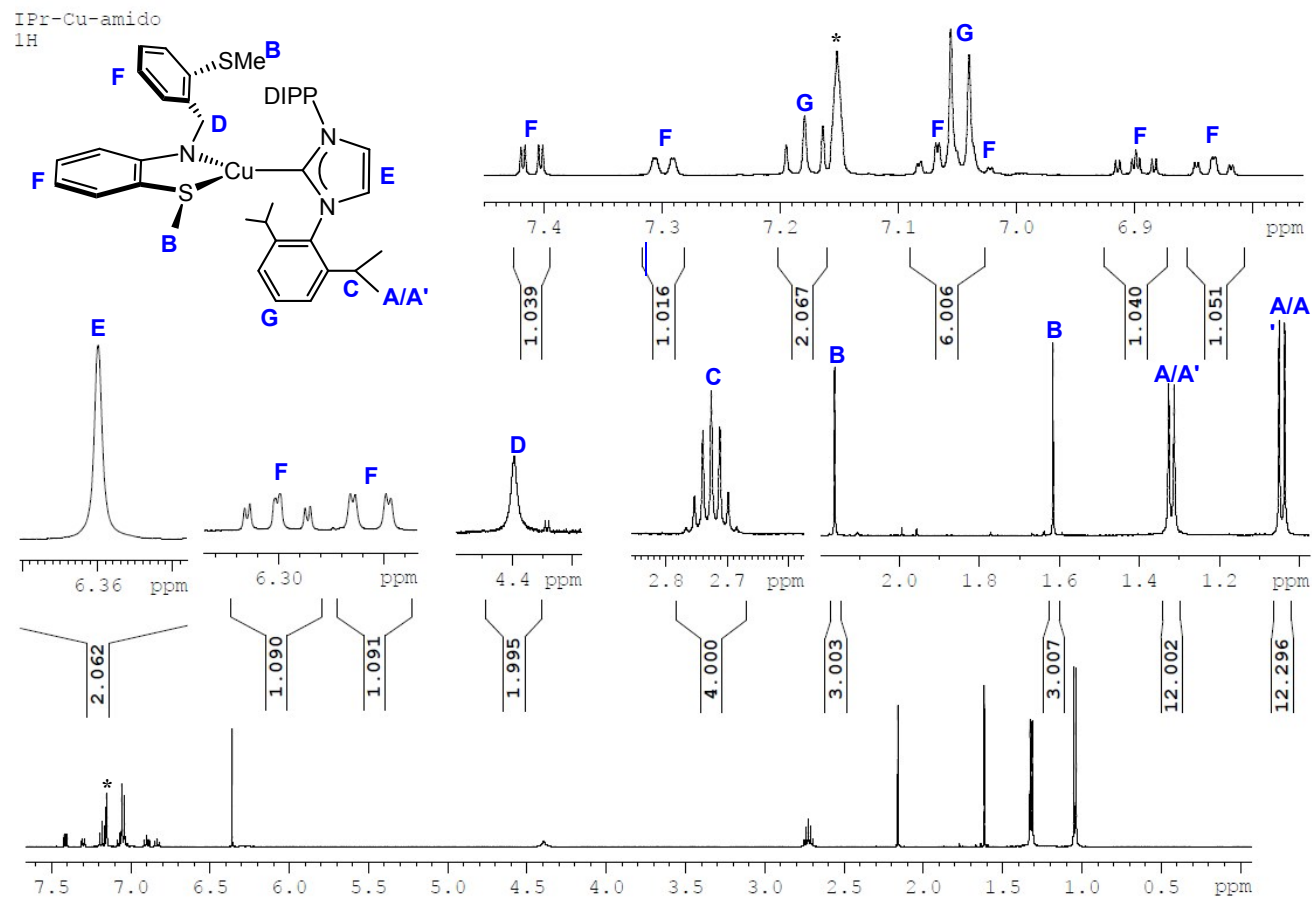


Figure S1. ¹H NMR spectrum of Cu(S^{Me}NS^{Me})(IPr) (Cu-1). * indicates C₆D₆.

IPr-Cu-amido
13C

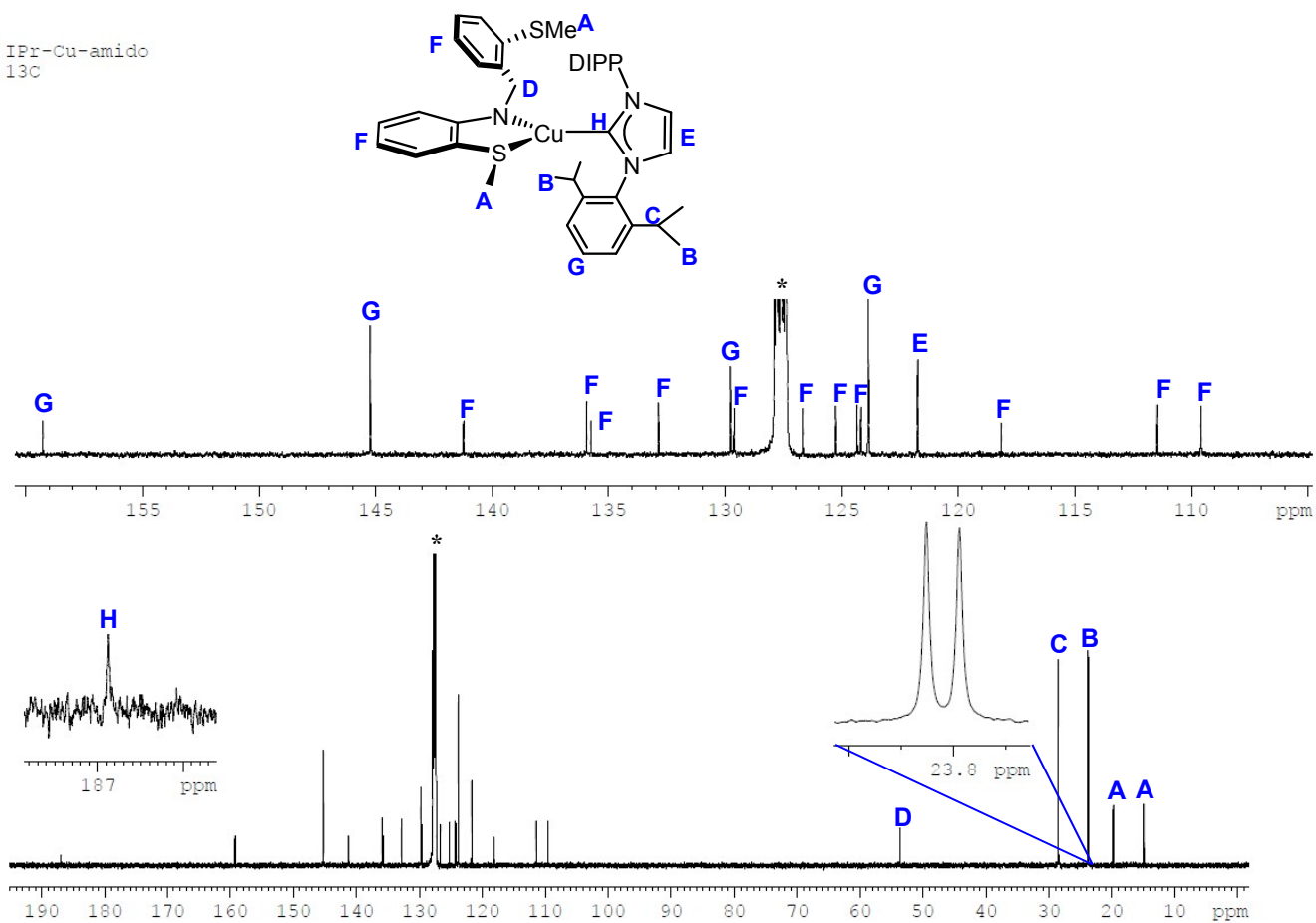


Figure S2. ¹³C{¹H} NMR spectrum of Cu(S^{Me}NS^{Me})(IPr) (**Cu-1**). * indicates C₆D₆.

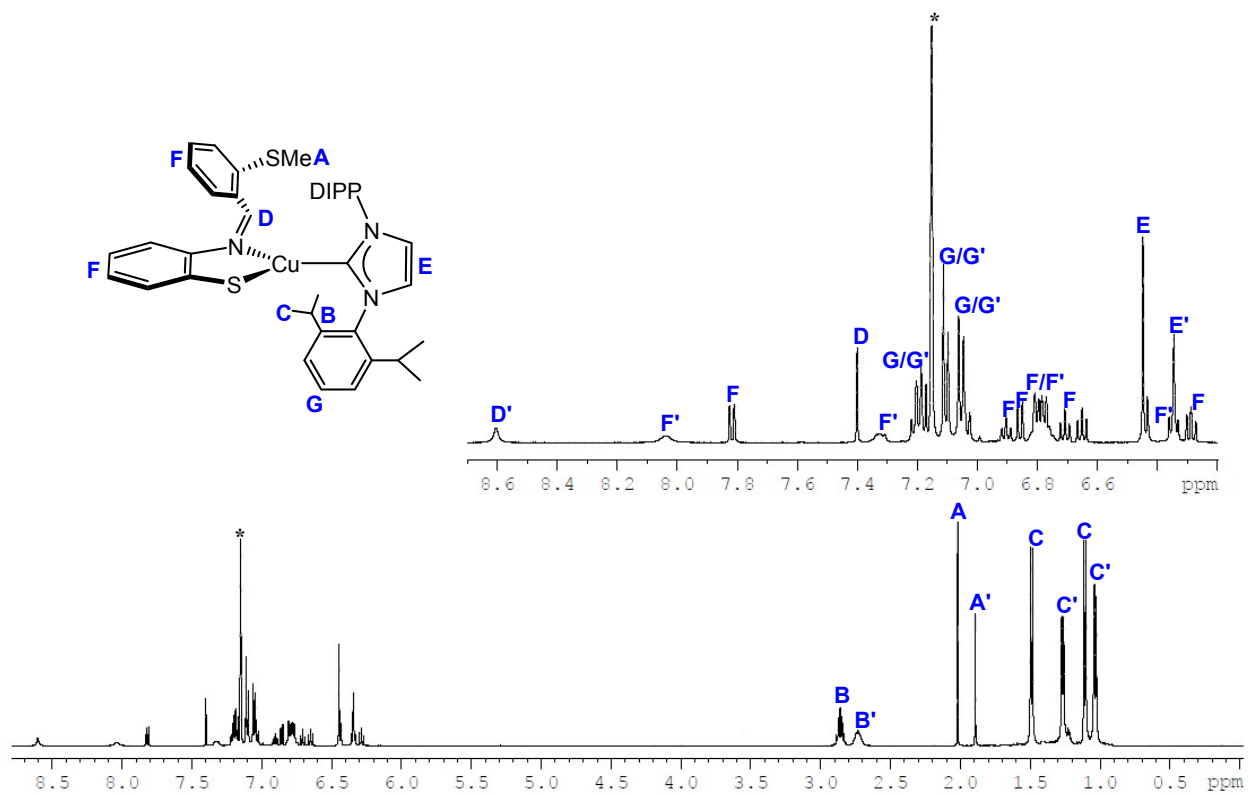


Figure S3. ^1H NMR spectrum of $\text{Cu}(\text{S}^{\text{Me}}\text{NS})(\text{IPr})$ (**Cu-2**). * indicates C_6D_6 .

IPr-Cu-thiolate
13C

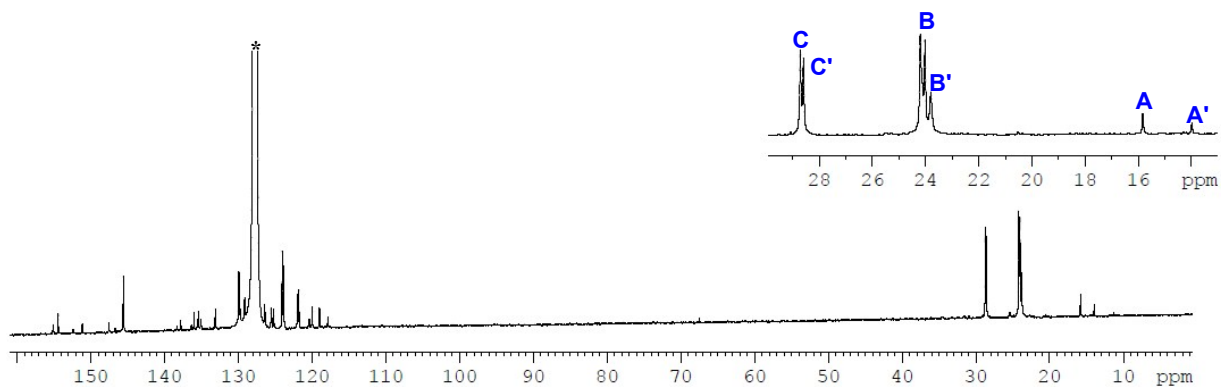
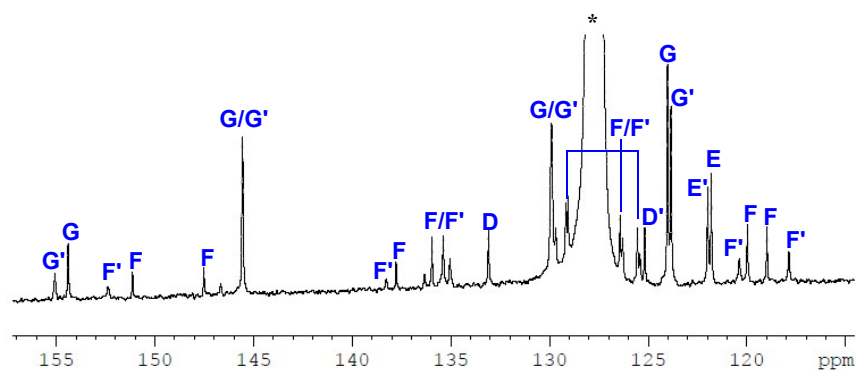
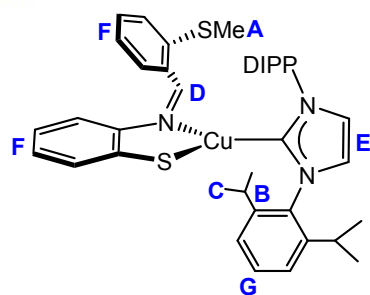


Figure S4. $^{13}\text{C}\{^1\text{H}\}$ NMR spectrum of $\text{Cu}(\text{S}^{\text{Me}}\text{NS})(\text{IPr})$ (**Cu-2**). * indicates C_6D_6 .

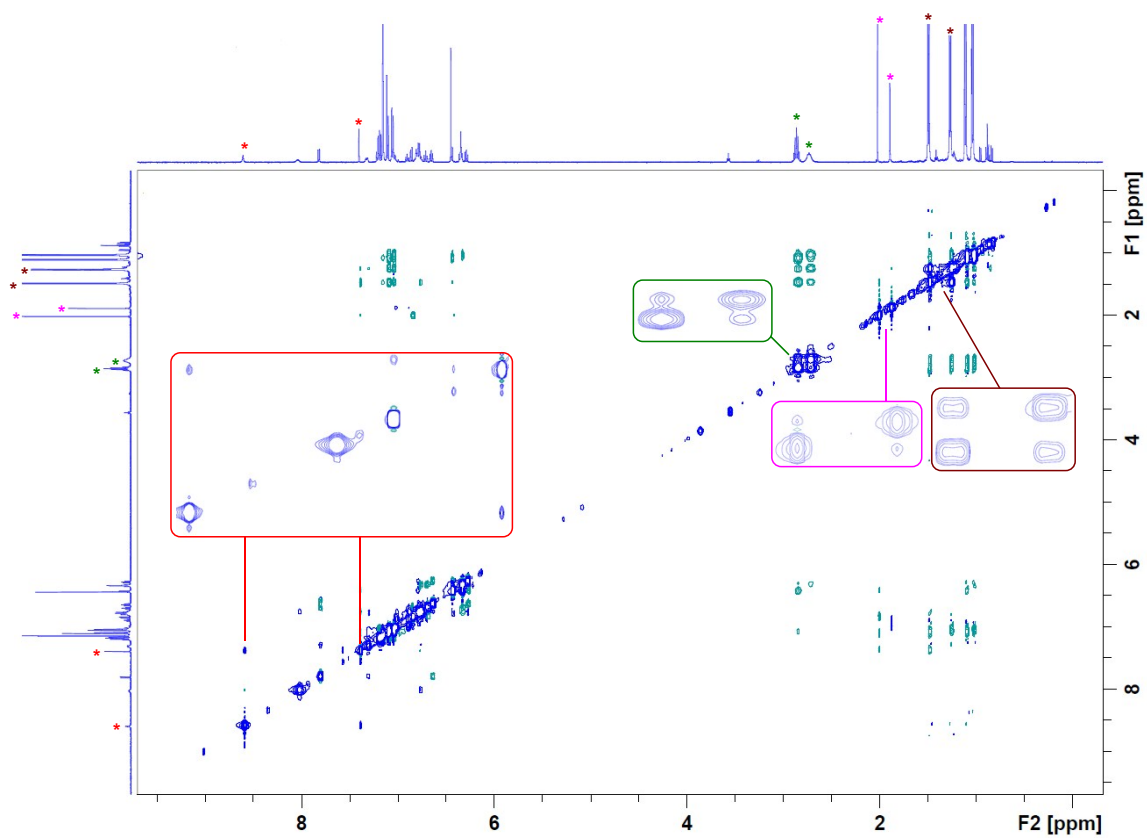


Figure S5. 2D ^1H EXSY NMR spectrum of $\text{Cu}(\text{S}^{\text{Me}}\text{NS})(\text{IPr})$ (**Cu-2**).

benzaldehyde hydroboration product
1H NMR

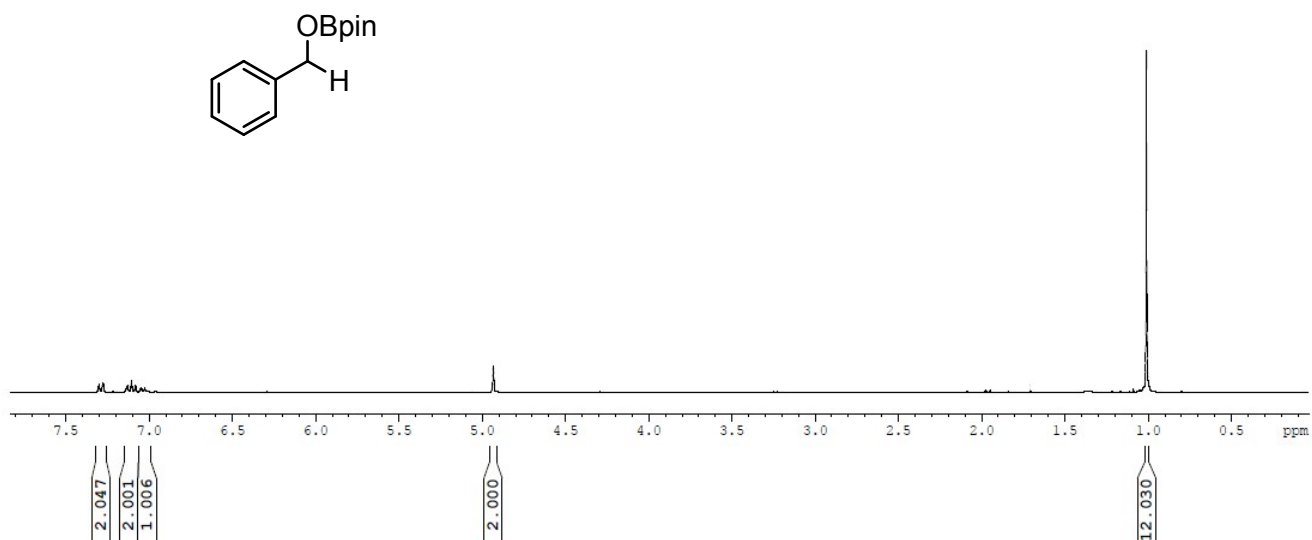


Figure S6. ^1H NMR spectrum of benzaldehyde hydroboration product. * indicates C_6D_6 .

acetophenone hydroboration product
1H NMR

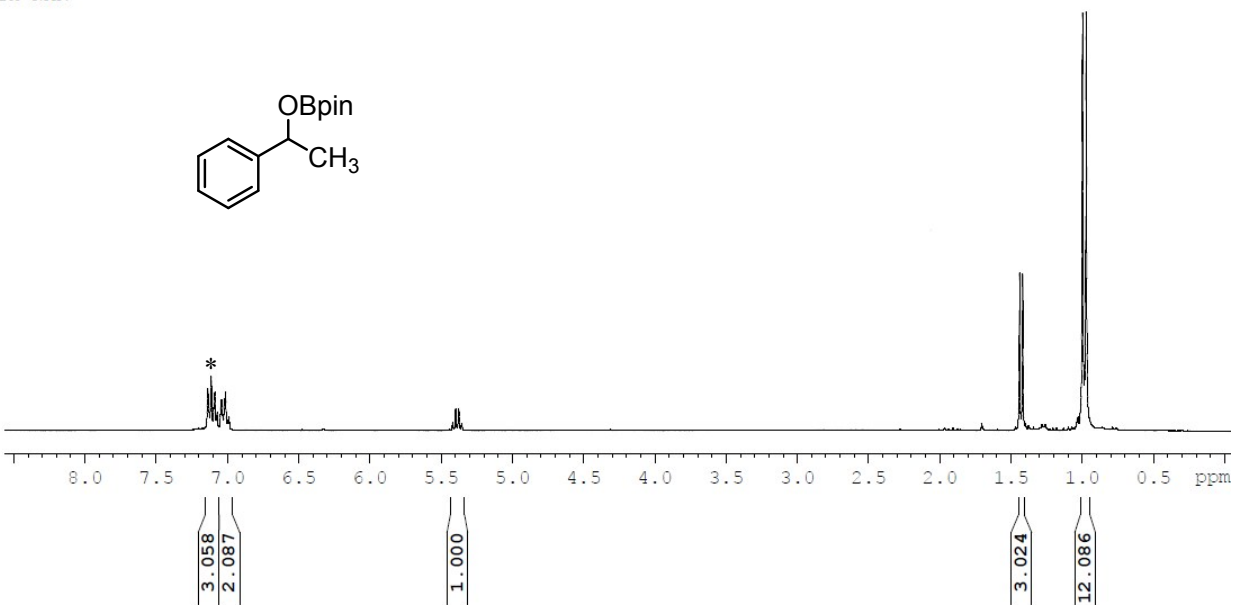


Figure S7. ^1H NMR spectrum of acetophenone hydroboration product * indicates C_6D_6 .

benzophenone hydroboration
1H

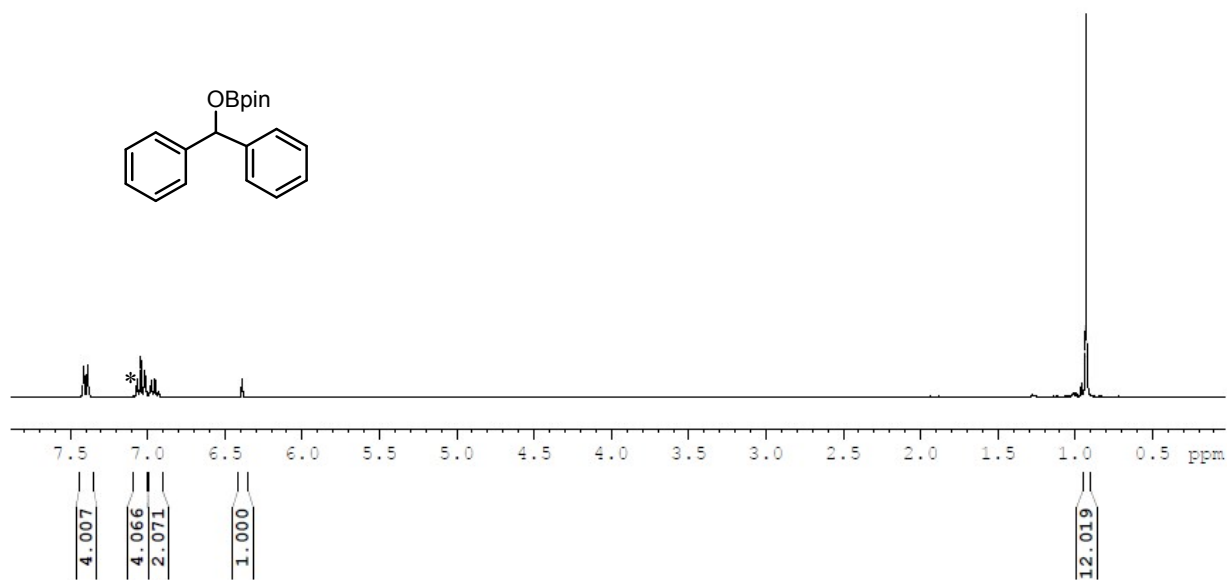


Figure S8. ¹H NMR spectrum of benzophenone hydroboration product * indicates C₆D₆.

benzaldehyde hydrosilylation product
1H NMR

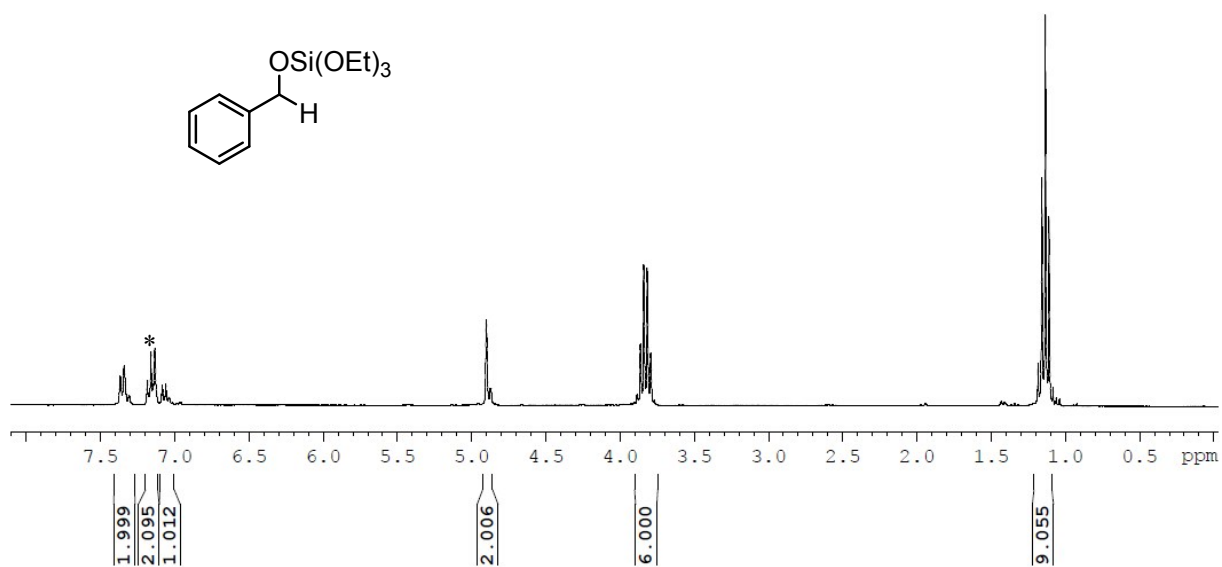


Figure S9. ¹H NMR spectrum of benzaldehyde hydrosilylation product * indicates C₆D₆.

trans-cinnamaldehyde hydrosilylation
1H

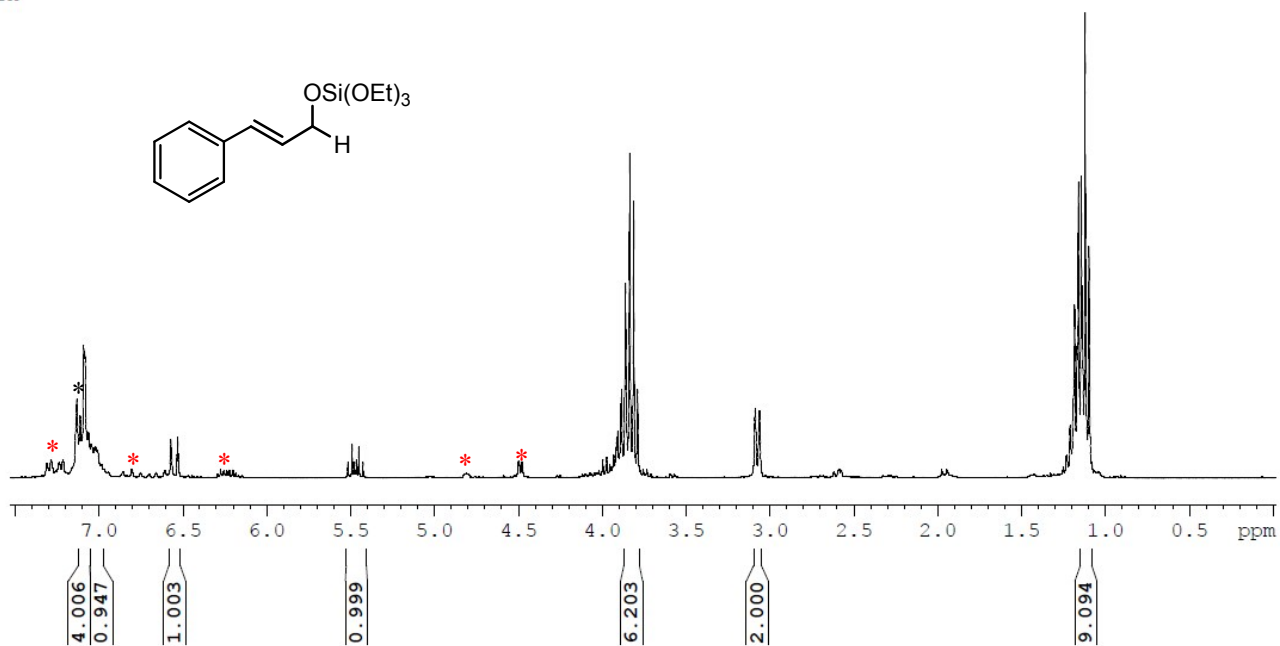


Figure S10a. ¹H NMR spectrum of *trans*-cinnamaldehyde hydrosilylation product. * indicates C_6D_6 . * indicates unknown impurity.

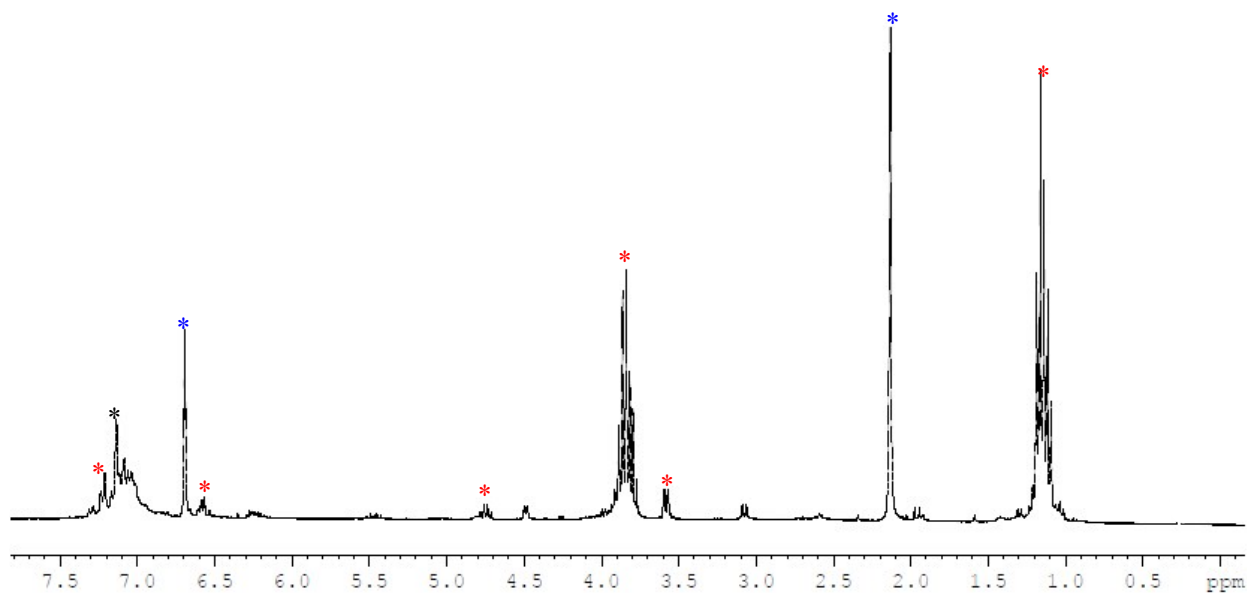


Figure S10b. ¹H NMR spectrum of *trans*-cinnamaldehyde hydrosilylation reaction mixture after 24 h. * indicates C_6D_6 . * indicates *cis*-product. * indicated internal standard mesitylene.

acetophenone hydrosilylation product
1H NMR

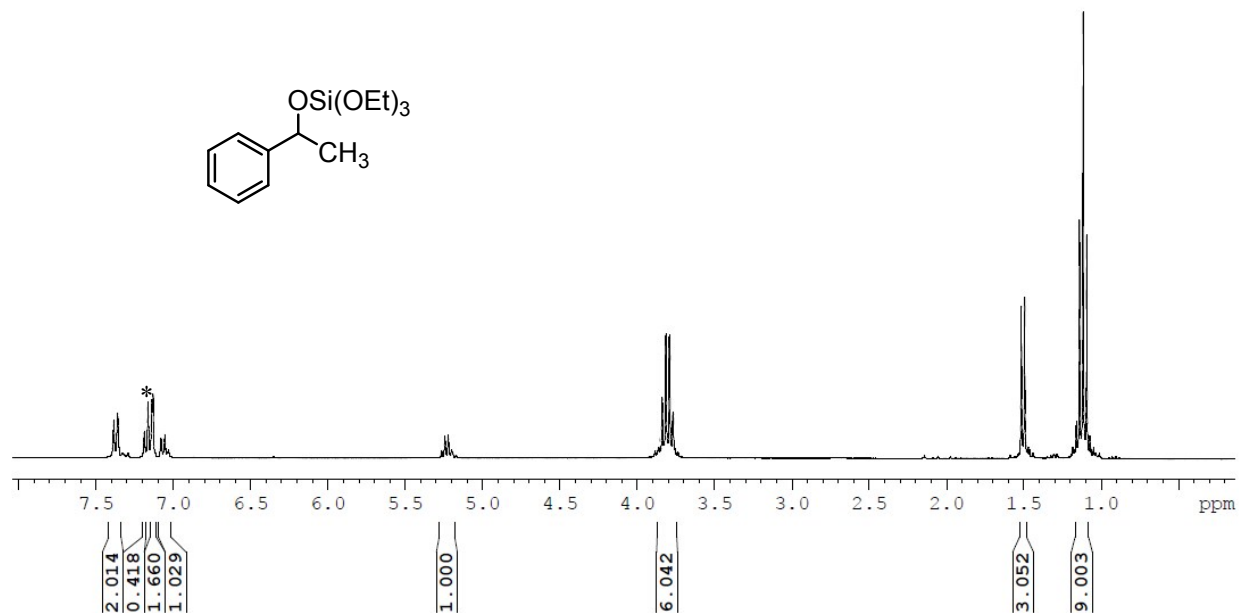


Figure S11. ^1H NMR spectrum of acetophenone hydrosilylation product. * indicates C_6D_6 .

benzophenone hydrosilylation
1H

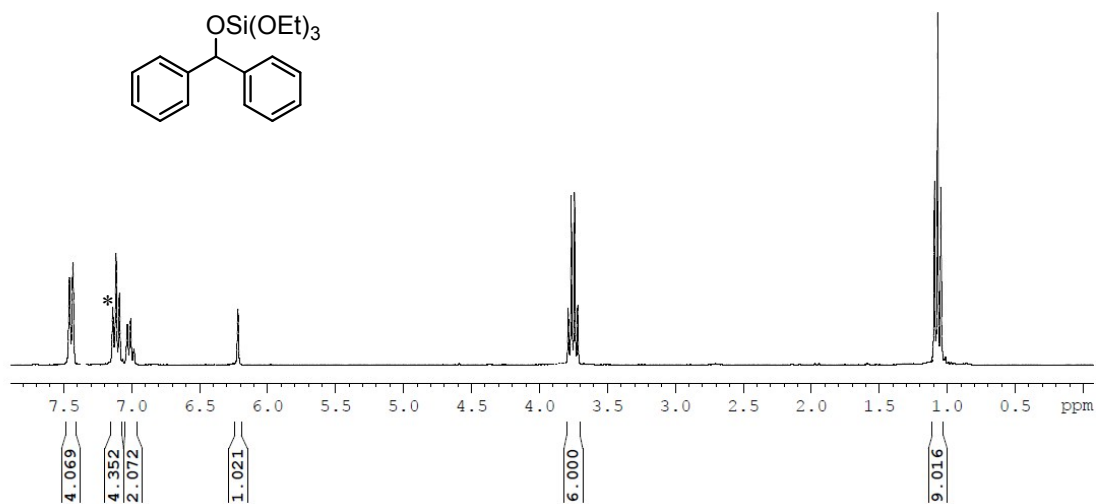


Figure S12. ^1H NMR spectrum of benzophenone hydrosilylation product. * indicates C_6D_6 .

5-hexen-2-one hydrosilylation
1H

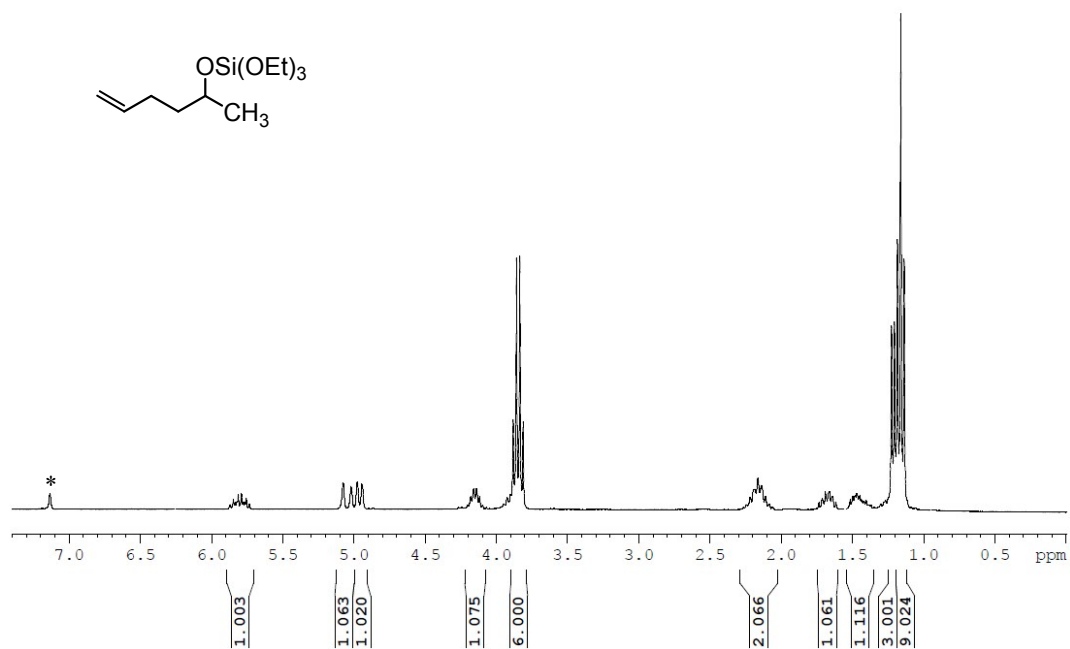


Figure S13. ^1H NMR spectrum of 5-hexen-2-one hydrosilylation product. * indicates C_6D_6 .

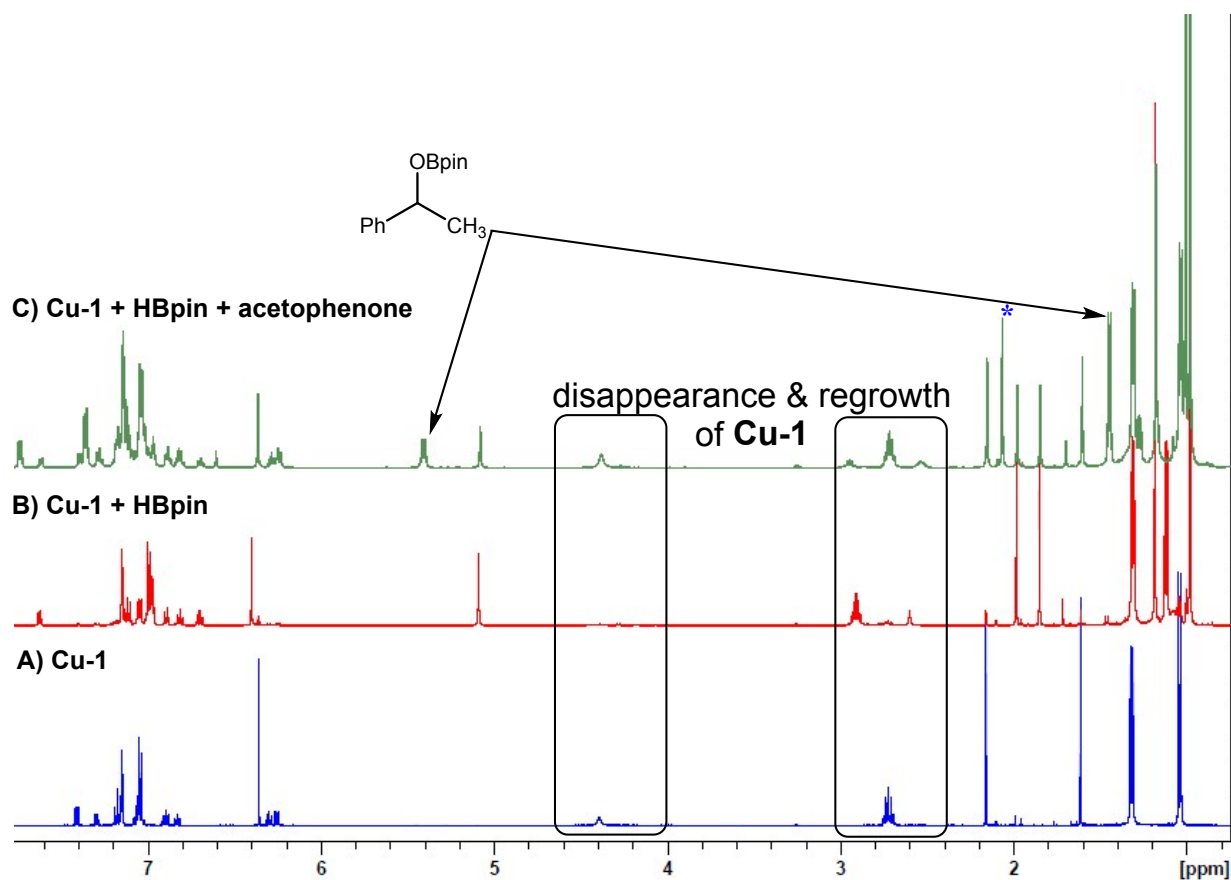


Figure S14. Stacked plot of ^1H NMR spectra showing stoichiometric conversion from A) **Cu-1** to B) Cu–H intermediate, and C) subsequent conversion to hydroboration product, reforming **Cu-1**.

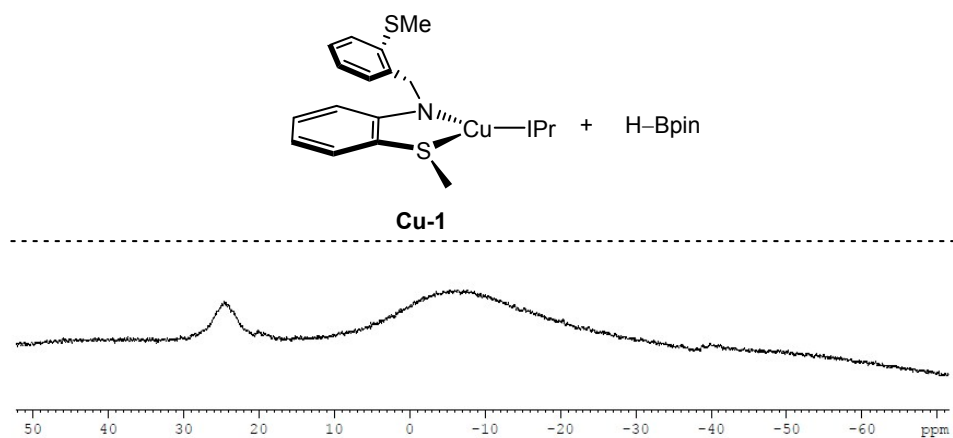


Figure S15. ^{11}B NMR spectra showing stoichiometric reaction of **Cu-1** with pinacolborane.

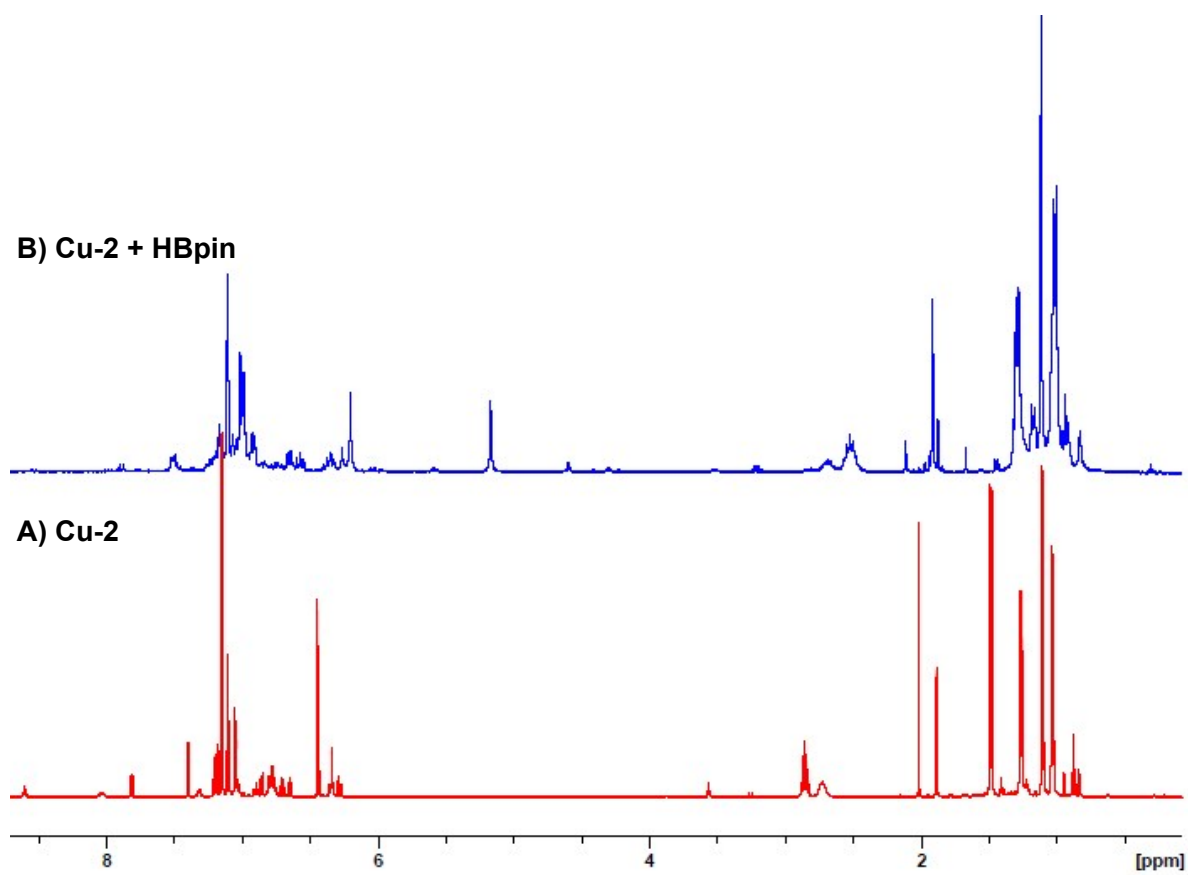


Figure S16. Stacked plot of ^1H NMR spectra showing stoichiometric reaction of **Cu-2** with pinacolborane.

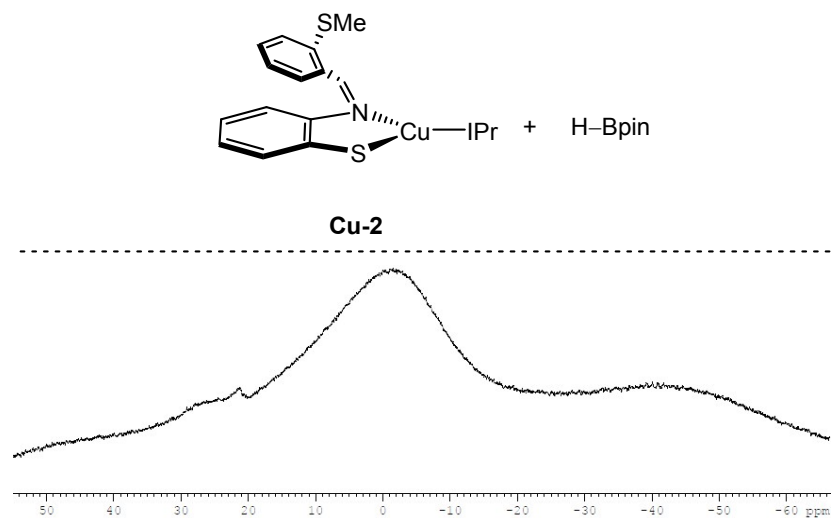


Figure S17. ^{11}B NMR spectra showing stoichiometric reaction of **Cu-2** with pinacolborane.

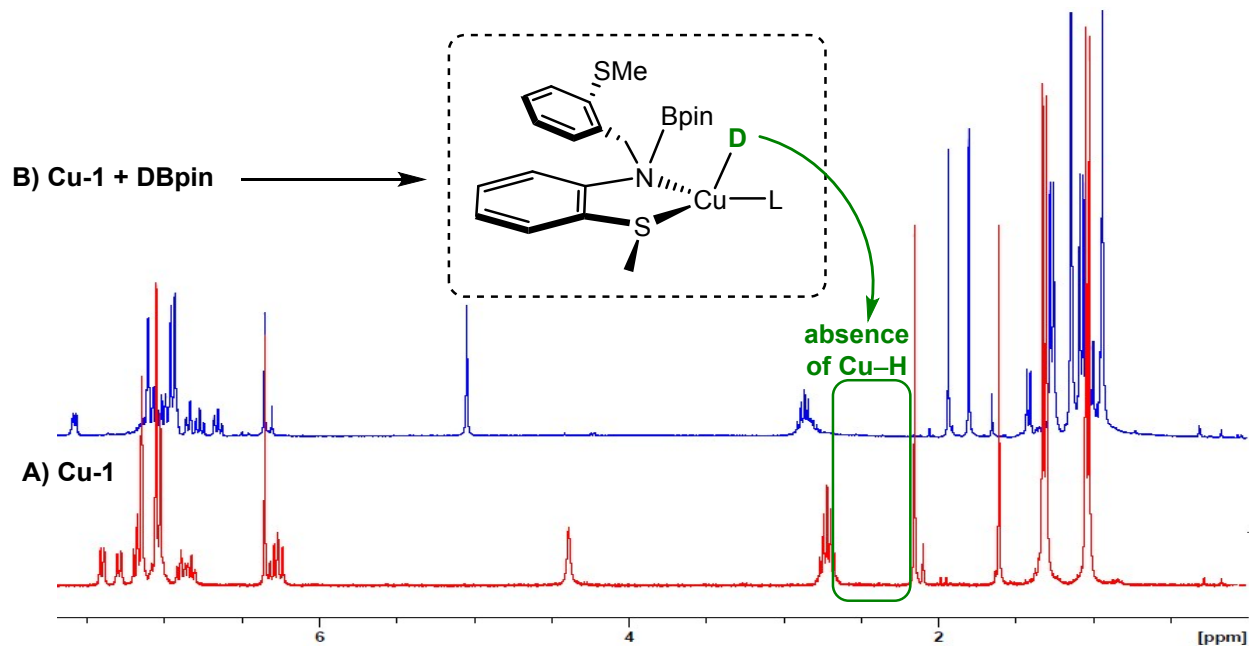


Figure S18. ^1H NMR spectrum of reaction of **Cu-1** with DBpin.

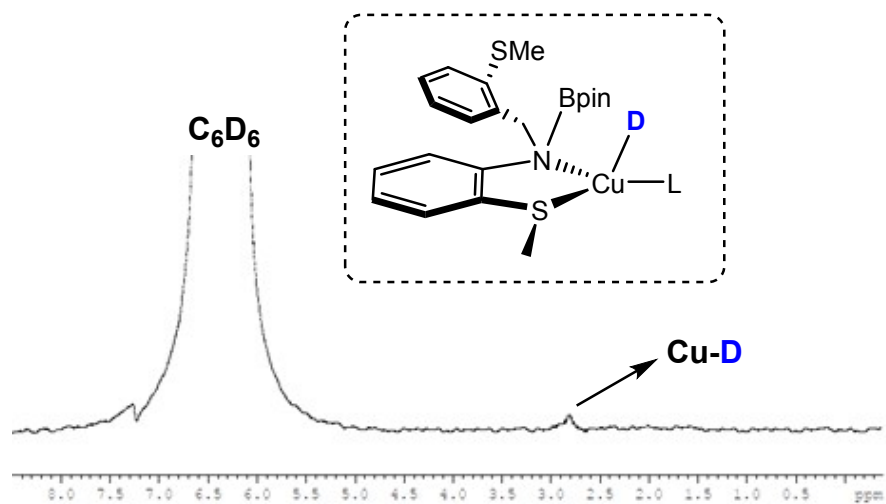


Figure S19. ^2H NMR spectrum of reaction of **Cu-1** with DBpin.

General Details: X-ray diffraction

The crystals were mounted on thin glass fibers using paraffin oil or cyanoacrylate glue. The crystals of **Cu-1** and **Cu-2** were cooled to 200 ± 2 K during data collection. The data was collected on Bruker single-crystal diffractometer equipped with a sealed Mo tube source (wavelength 0.71073 Å) and APEX II CCD detector. The raw data collection and processing were performed with Bruker APEX II software package.¹⁸ Semi-empirical absorption correction based on equivalent reflections were applied.¹⁹ Systematic absences and unit cell parameters were consistent with monoclinic $P2_1$ (#4) for **Cu-1**, monoclinic $P2_1/c$ (#14) for **Cu-2**.

The structures were solved by intrinsic phasing and refined with full-matrix least-squares procedure based on F^2 , using SHELXL.²⁰ All non-hydrogen atoms were refined anisotropically. The hydrogen atoms bonded to carbon atoms were placed in idealized positions.

Refinement details for Cu-1.

Due to the value of the Flack parameter [0.463(9)], a centrosymmetric space group was considered ($P21/m$), however a satisfactory structure solution was not obtained. The Flack value is therefore attributed to an inverse twin, for which the following Twin Law was applied:

TWIN -1 0 0 0 -1 0 0 0 -1

BASF 0.463

Two isopropyl carbons displayed disorder, each with 0.5 occupancy. The SADI and RIGU restraints were applied to C40, C41A, C42A, C41B, and C42B.

Refinement details for Cu-2.

The structure was refined without additional restraints/constraints. No disorder was present.

Table S2. Crystal data and structure refinement for IPr-Cu-amido (Cu-1).

Identification code	IPr-Cu-amido
Empirical formula	C ₄₂ H ₅₂ CuN ₃ S ₂
Formula weight	726.52
Temperature/K	200.05
Crystal system	monoclinic
Space group	P2 ₁
a/Å	12.471(8)
b/Å	13.794(9)
c/Å	13.094(8)
α/°	90
β/°	116.562(16)
γ/°	90
Volume/Å ³	2015(2)
Z	2
ρ _{calc} /g/cm ³	1.198
μ/mm ⁻¹	0.677
F(000)	772.0
Crystal size/mm ³	0.1 × 0.05 × 0.05
Radiation	MoKα (λ = 0.71073)
2θ range for data collection/°	3.478 to 56.164
Index ranges	-15 ≤ h ≤ 16, -17 ≤ k ≤ 18, -17 ≤ l ≤ 17
Reflections collected	26692
Independent reflections	9542 [R _{int} = 0.0276, R _{sigma} = 0.0312]
Data/restraints/parameters	9542/40/465
Goodness-of-fit on F ²	1.050
Final R indexes [I >= 2σ (I)]	R ₁ = 0.0299, wR ₂ = 0.0706
Final R indexes [all data]	R ₁ = 0.0345, wR ₂ = 0.0731
Largest diff. peak/hole / e Å ⁻³	0.45/-0.17
Flack parameter	0.463(9)

Table S3. Bond Lengths for IPr-Cu-amido (Cu-1).

Atom	Atom	Length/Å	Atom	Atom	Length/Å
Cu1	S1	2.4820(14)	C8	C9	1.554(4)
Cu1	N1	1.948(2)	C3	C4	1.396(5)
Cu1	C16	1.919(3)	C9	C10	1.397(4)
S1	C2	1.803(3)	C9	C14	1.421(4)
S1	C1	1.832(4)	C18	C17	1.351(3)
S2	C14	1.787(3)	C7	C6	1.452(4)
S2	C15	1.826(4)	C33	C34	1.397(4)
N3	C19	1.456(3)	C25	C27	1.551(4)
N3	C16	1.382(3)	C25	C26	1.544(5)
N3	C18	1.406(3)	C24	C23	1.403(4)
N2	C31	1.465(3)	C24	C28	1.552(4)
N2	C16	1.377(3)	C10	C11	1.410(5)
N2	C17	1.404(3)	C37	C39	1.548(5)
N1	C8	1.467(3)	C37	C38	1.531(5)
N1	C7	1.369(3)	C21	C22	1.395(4)
C20	C19	1.423(4)	C40	C42B	1.564(8)
C20	C25	1.543(4)	C40	C41B	1.512(8)
C20	C21	1.401(4)	C40	C41A	1.587(10)
C31	C36	1.415(3)	C40	C42A	1.514(10)
C31	C32	1.415(3)	C14	C13	1.423(5)
C19	C24	1.420(3)	C23	C22	1.396(5)
C36	C35	1.413(4)	C28	C30	1.539(4)
C36	C40	1.546(4)	C28	C29	1.546(5)
C32	C33	1.413(4)	C11	C12	1.387(6)
C32	C37	1.533(4)	C4	C5	1.389(5)
C35	C34	1.397(4)	C6	C5	1.396(4)
C2	C3	1.406(4)	C13	C12	1.394(6)
C2	C7	1.437(4)			

Table S4. Crystal data and structure refinement for IPr-Cu-thiolate (Cu-2).

Identification code	IPr-Cu-thiolate
Empirical formula	C ₄₁ H ₄₈ CuN ₃ S ₂
Formula weight	710.48
Temperature/K	298.15
Crystal system	monoclinic
Space group	P2 ₁ /n
a/Å	12.955(3)
b/Å	15.654(3)
c/Å	19.260(4)
α/°	90
β/°	95.175(13)
γ/°	90
Volume/Å ³	3889.8(15)
Z	4
ρ _{calc} /g/cm ³	1.213
μ/mm ⁻¹	0.700
F(000)	1504.0
Crystal size/mm ³	0.382 × 0.18 × 0.179
Radiation	MoKα (λ = 0.71073)
2θ range for data collection/°	3.358 to 53.298
Index ranges	-13 ≤ h ≤ 16, -19 ≤ k ≤ 19, -24 ≤ l ≤ 24
Reflections collected	36950
Independent reflections	8089 [R _{int} = 0.0405, R _{sigma} = 0.0333]
Data/restraints/parameters	8089/0/433
Goodness-of-fit on F ²	1.011
Final R indexes [I >= 2σ (I)]	R ₁ = 0.0429, wR ₂ = 0.1005
Final R indexes [all data]	R ₁ = 0.0757, wR ₂ = 0.1161
Largest diff. peak/hole / e Å ⁻³	0.52/-0.26

Table S5. Bond Lengths for IPr-Cu-thiolate (Cu-2).

Atom	Atom	Length/Å	Atom	Atom	Length/Å
Cu1	S1	2.1802(8)	C39	C40	1.528(4)
Cu1	N1	2.130(2)	C39	C41	1.513(5)
Cu1	C15	1.889(2)	C31	C36	1.508(4)
S1	C1	1.743(3)	C31	C32	1.385(4)
S2	C13	1.751(3)	C23	C27	1.503(5)
S2	C14	1.752(4)	C23	C22	1.391(4)
N2	C18	1.446(3)	C24	C25	1.522(4)
N2	C15	1.367(3)	C24	C26	1.517(5)
N2	C17	1.371(3)	C7	C8	1.470(4)
N3	C30	1.446(3)	C8	C13	1.383(4)
N3	C15	1.350(3)	C8	C9	1.375(4)
N3	C16	1.382(3)	C13	C12	1.376(4)
N1	C6	1.416(3)	C36	C38	1.501(4)
N1	C7	1.275(3)	C36	C37	1.501(4)
C18	C19	1.385(4)	C27	C28	1.529(4)
C18	C23	1.383(3)	C27	C29	1.523(5)
C30	C35	1.399(4)	C5	C4	1.368(5)
C30	C31	1.381(4)	C12	C11	1.361(5)
C17	C16	1.326(4)	C20	C21	1.369(5)
C19	C24	1.496(4)	C2	C3	1.372(6)
C19	C20	1.394(4)	C9	C10	1.362(5)
C1	C6	1.380(4)	C34	C33	1.361(5)
C1	C2	1.384(4)	C32	C33	1.358(5)
C35	C39	1.501(4)	C10	C11	1.357(5)
C35	C34	1.394(4)	C22	C21	1.348(5)
C6	C5	1.395(4)	C4	C3	1.358(7)

References

- 1) M. Espinal-Viguri, S. E. Neale, N. T. Coles, S. A. Macgregor, and R. L. Webster, *J. Am. Chem. Soc.* 2019, **141**, 1, 572-582.
- 2) H. Sakaguchi, Y. Uetake, M. Ohashi, T. Niwa, S. Ogoshi, and T. Hosoya, *J. Am. Chem. Soc.* 2017, **139**, 12855-12862.
- 3) U. K. Das, S. L. Daifuku, T. E. Iannuzzi, S. I. Gorelsky, I. Korobkov, B. Gabidullin, M. L. Neidig, and R. T. Baker, *Inorg. Chem.* 2017, **56**, 13766-13776.
- 4) U. K. Das, S. L. Daifuku, S. I. Gorelsky, I. Korobkov, M. L. Neidig, J. L. Le Roy, M. Murugesu, and R. T. Baker, *Inorg. Chem.* 2016, **55**, 987-997.
- 5) M. Arrowsmith, T. J. Hadlington, M. S. Hill, and G. Kociok-Kohn, *Chem. Commun.* 2012, **48**, 4567-4569.
- 6) E. Peterson, A. Y. Khalimon, R. Simionescu, L. G. Kuzmina, J. A. K. Howard, and G. I. Nikonov, *J. Am. Chem. Soc.* 2009, **131**, 908-909.
- 7) S. Vijjamarrri, V. K. Chidara, J. Rousova, and G. Du, *Catal. Sci. Technol.* 2016, **6**, 3886-3892.
- 8) S. Keess, A. Simonneau, and M. Oestreich, *Organometallics*, 2015, **34**, 790-799.
- 9) C. Boone, I. Korobkov, and G. I. Nikonov, *ACS. Catal.* 2013, **3**, 10, 2336-2340.
- 10) R. M. Coates, P. D. Senter, and W. R. Baker, *J. Org. Chem.* 1982, **47**, 3597-3607.
- 11) B. H. Lipshutz, W. Chrisman, and K. Noson, *Organomet. Chem.* 2001, **624**(1-2), 367-371.
- 12) S. Sirol, J. Courmarcel, N. Mostefai, and O. Riant, *Org. Lett.* 2001, **3**(25), 4111-4113.
- 13) H. Kaur, F. K. Zinn, E. D. Stevens, and S. P. Nolan, *Organometallics* 2004, **23**(5), 1157-1160.
- 14) S. Díez-González, H. Kaur, F. K. Zinn, E. D. Stevens, and S. P. Nolan, *J. Org. Chem.* 2005, **70**(12), 4784-4796.
- 15) S. Díez-González, N. M. Scott, and S. P. Nolan, *Organometallics* 2006, **25**(9), 2355-2358.
- 16) T. Vergote, F. Nagra, A. Welle, M. Luhmer, J. Wouters, N. Mager, and T. Leyssens, *Chem. Eur. J.* 2012, **18**(3), 793-798.
- 17) D. W. Lee and J. Yun, *Tet. Lett.* 2004, **45**, 5415-5417.
- 18) APEX 2, Bruker AXS Inc., Madison, Wisconsin, USA, 2012
- 19) G. M. Sheldrick, SADABS, Program for empirical absorption correction of area detector data, University of Göttingen, Germany, 1996.
- 20) G. M. Sheldrick, *Acta Cryst.* 2015, **C71**, 3-8.